DD

GANIL

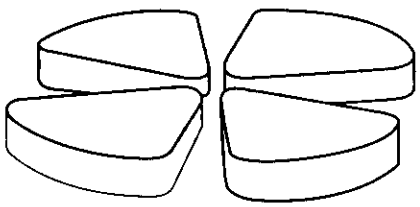

Status of the VAMOS Spectrometer at GANIL

presented by Rémy ANNE,

VAMOS project leader,
GANIL, BP 5027, 14076 Caen Cedex 5, France,

for the VAMOS Collaboration,

at the " EXON – 2001" International Symposium on Exotic Nuclei,
Baikal lake, Irkutsk, 24-28 July 2001

GANIL P 02 02

Status of the VAMOS Spectrometer at GANIL

presented by Rémy ANNE

for the VAMOS collaboration

1. History

The VAMOS spectrometer (achronym for VAriable MOde Spectrometer) is intended to cover experimental needs associated with the study of nuclear reactions using as projectiles the new radioactive beams delivered by the GANIL-SPIRAL facility. It has been studied and constructed by a group of European laboratories.

The project started by a European contract of research and development obtained in 1996 and running until 1999. This contract for R&D funds was signed by different institutes, GANIL Caen, GSI Darmstaad, CCLRC Daresbury, the Universities of Liverpool and Surrey. Later on other laboratories joined the project for both the studies and the construction phases: CEN Bordeaux, DAPNIA/SPHN Saclay, IPN Orsay, LPC Caen, NPI Prague and the Universities of Giessen and Manchester.Three main meetings gathering around one hundred participants were organized in order to list the physics motivations, followed by a ten of technical ones involving around 20 participants in order to define the different components. A M.O.U was signed in 1998 between all the above-mentioned laboratories and the project was organized through eight working groups, (ref 1). Studies and construction took place during the 1998 to 2000 years and the mounting was achieved in July 2001.

2. Generalities

The aim of the present paper is to present the status of the VAMOS spectrometer which construction is quite achieved at GANIL and to emphasize particularly some points which needed significant efforts in the research and development field such as, the corrections of the large optical aberrations due to the wide angular aperture of the spectrometer, the technical developments on the velocity filter and finally the low matter secondary electron detector (SED) needed and developed for the trajectories reconstruction of the very low energy heavy ions.

3. The physics motivations

I shall briefly recall the physics, which was the motive for the construction of this spectrometer

For each reaction type, an experimental setup involving the spectrometer and ancillary detectors was imagined in order to define the characteristics and properties the spectrometer and its associated detection should have, and finally deduce the technical specifications for each element.

The following mechanisms are to be studied: peripheral collisions, deep inelastic collisions, and fusion-evaporation reactions.

3.1 Peripheral collisions:

Elastic and inelastic scattering in reverse kinematics and reverse kinematics transfer reactions type : A(p, p'), A(d, p). A is the projectile and p or d the target.
In these cases of interest:

The light particles are detected in a multi-detector, (like MUST), located around the target point, in coincidence with the focal plane of the spectrometer.

The maximum useful angle is below 10 degrees

The energy of the ejectile is typically 5 to 20 MeV/u

The mass M and the atomic number Z must be identified

The direct beam must be eliminated

3.2 Deep inelastic collisions:

The aim is double, to produce new nuclei and to study the N /Z ratio equilibration as a function of isospin.
For these two purposes:

A very wide solid angle spectrometer is desirable.

The energy of the reaction products is 1 to 5 MeV/u

Detection angles up to 90 degrees are necessary.

The mass M and the neutron number N are to be identified with M values often above 100.

3.3 Fusion-evaporation reactions:

New proton or neutron rich nuclei are accessible and are to be produced in direct kinematics. The low energy residues will be identified by coincidence with prompt radiations detected by detectors located around the target, like EXOGAM, or with delayed ones, (gamma, protons, neutrons, fissions products) detected in implantation-disintegrations counters located in the focal plane.
For these studies: :

A wide solid angle, 5 to 10 degrees, is needed

M/Q identification is required

The energy of the reaction products is low, 0.1 to 1 MeV/u

The rejection of the incident beam is necessary.

4. Spectrometer characteristics

Taking into account the low intensity of the secondary beams delivered by the new accelerator SPIRAL in comparison with the high one actually delivered by GANIL cyclotrons, and in order to meet the above mentioned requirements, the spectrometer has in summary the following main characteristics:

A very large geometrical acceptance, around 85 msr, (+ / - 140 mr angular aperture in the two planes).

A nominal dispersion, about 2.5 cm / % at the focal plane location, in good agreement with the resolution that can be obtained by using the new developed focal plane detectors.

A momentum acceptance of + /- 5 %

A velocity filter function.

In addition the whole ensemble can be rotated around the target point from 0 to 100 degrees, and enough place around the target is preserved in order to install large detectors in coincidence with the focal plane detection.

These characteristics are obtained in the following optical structure (see fig 1):

Two large aperture quadrupoles, which provide the large geometrical acceptance. The first has a 30 cm diameter and a magnetic length of 60 cm, while the second is elliptical with a 1.0 m long main axis (horizontal) and a 90 cm magnetic length.

A variable angle dipole (nominal radius 1.5 m, gap 20 cm), from 0 to 60 degrees, which permits to set the required dispersion,

A 1.0 m long Wien filter for providing the velocity selection.

The technical characteristics of all the elements and general informations can be found in ref.2

In addition, the object distance between the target point and the first quadrupole is variable, from 40 cm to 150 cm . Two reasons for this variable distance : first one, the necessity to preserve a large place for big target chambers or big detectors installed around the target point, secondly, the possibility to accept higher magnetic rigidities nuclei in the optical structure. For the shorter 40 cm distance, the acceptance of the spectrometer is around 85 msr and the maximum magnetic rigidity 1.6 T.m, while for the 150 cm distance the acceptance is still around 30 msr and the BR increased to 2.3 T.m.

In summary, this means that the whole spectrometer is installed on two superposed platforms, a first upper one which can be translated along the beam direction over a 110 cm variable distance, moving over a second lower one, which can be rotated from 0 to 100 degrees.

5. Operation

The originality of such a spectrometer is that depending on the coupling of the different optical elements, quadrupoles, dipole, velocity filter, it provides several optimized operating modes adapted to the diversity of experiments,

We can consider three main operating modes:

Mode	Elements	In operation	Function
1	Quadrupoles Dipole Velocity filter	Yes No No	Wide acceptance facility
2	Quadrupoles Dipole Velocity filter	Yes Yes No	Wide acceptance, dispersive spectrometer
3	Quadrupoles Dipole Velocity filter	Yes Yes Yes	Dispersive spectrometer and / or M / Q resolution with beam rejection

6. Some elements of Optics.

The nominal first order matrix M from the target to the focal plane, for a 1.5 m focal length and a 60 degrees analyzing angle is the following:

$(x_f \ \theta_f \ y_f \ \Phi_f, \ l_f \ dp/p) = M \ (x_i, \theta_i \ y_i \ \Phi_i \ l_i \ dp/p_i)$.
(Transport units: cm, mr, m and %).

-1.049752	0.0	0.0	0.0	0.0	2.479111
-1.241403	- 0.951752	0.0	0.0	0.0	1.153991
0.0	0.0	- 6.818949	0.0	0.0	0.0
0.0	0.0	2.619415	- 0.146419	0.0	0.0
1.861850	2.359104	0.0	0.0	1.0	0.273760
0.0	0.0	0.0	0.0	0.0	1.0

This first order matrix makes sense to estimate the size of the beam at the detectors location if the large aberrations inherent to a so large aperture spectrometer are cancelled or at least corrected and minimized.

6.1 Aberrations correction

Calculations have shown that the more important aberrations are geometrical ones (mainly the term x_i / θ_i^3) induced by the wide aperture quadrupôle Q2 which over focuses the large angle trajectories. For example, if we do calculations taking for Q2 a pure quadrupolar field and for the beam phase space a 1mm width and a + / - 160 mr divergence, the aberrations are higher than several tens of centimeters ! see fig 2, which shows the position x (meter) and angle t (radian) of the central 1.6 T.m trajectory in the focal plane.
Concerning the magnetic rigidity acceptance, can be seen on the same plot 2 the trajectories corresponding to 1.6 T.m + / - 5 % which correspond to the maximal acceptance. It is clearly seen that for positives angles the three trajectories are mixed and that the initial angles of trajectories cannot be univoquely determined even with a powerful trajectory reconstruction code. In other words there is no resolution.
To correct these aberrations, it is necessary to introduce high order field components, up to dodecapolar ones, (see fig 3 : theoretical multipolar corrections). Insertion of discrete multipoles elements in the structure would have been very difficult, quite impossible and at least very expensive taking into account the large dimensions of such multipoles magnets. Therefore, the optimal way consisted in shaping the poles of Q2 according to a law determined by iterative calculations using on one hand the code ZGOUBY which is a code of trajectories integration to calculate the aberrations and on the other hand TOSCA which is a 3 dimensions magnetic field predictive code (see ref. 3)
The final law obtained for the pole shape is represented on fig 4. It shows the mechanical corrections to be brought to the reference hyperbolic gap of a pole giving a pure quadrupolar field.

The efficiency of such a pole profile shaping on the aberrations can be seen on fig 5 a where we can see the corrected trajectories corresponding to BR = 1.6 T.m + / - 1., 2., 3., 4., 5. %. Let us notice that these corrections do not affect the vertical movement, the vertical beam size being very small compared to the + / - 50 cm horizontal one.

A first test using a 3 energies alpha source (5.1575, 5.4865, 5.806 MeV) and the full angular acceptance has been achieved in July and September corresponding to dBR / BR0 = - 3.0 %, 0.0 %, and + 2.91 %. These first preliminary results plotted on fig 5 b look very close to the simulations and are therefore very promising. They confirm if necessary the good predictivity of the TOSCA code.

6.2 Velocity filter.

In order to reject the primary beam or to use the spectrometer in an A / Q selection mode, a velocity filter has been inserted in the optical structure. This velocity filter can be seen on photo. 1. It was the object of a huge technical research and development because of its particular configuration (see ref.4.) The difficulty is that, in the useful volume of the filter (1m x 1m x 0.15 m), the electrostatic field is parallel to the large horizontal dimension , one meter, and not to the short one 0.15 m. In consequence, to insure a good field homogeneity, the 300 kV high voltage needs to be distributed by means of two planes of electrodes, two nets of fifteen, inter-connected by high voltage resistors each associated which a spark gap in order to prevent from electric discharges. The field configuration can be observed on fig 6.

7. Detection.

The large aberrations being corrected, it is nevertheless necessary to have good resolution detectors in order to reconstruct the trajectories, i e to determine for each ion its magnetic rigidity and its initial horizontal and vertical emission angles at the target exit. The standard detection set up is shown on fig 7. In all cases, light or heavy ions, fast or slow ions, two position measurements in each plane are necessary, upstream and downstream the tilted focal plane, associated with energy loss, energy and time measurements to identify the atomic number and the mass.

The standard detection for the light and fast ions consists in two drift chambers, an ionization chamber and a plastic.

For the medium and heavy slow ions, the drift chambers are replaced by two Secondary Emission Detectors (SED) and, depending on the energy of the ions the ionization chamber provides a measurement of the energy loss or the total energy, while the time signal is taken from the plastic or the SED (see ref. 5).

The SED consists in a thin 45 ° tilted foil located on the trajectory of the ions, see fig 8. Under the impact of the ions to be detected, the foil emits secondary electrons, which drift for collection over a 20 cm distance through a 10 keV high voltage onto a planar detector located on the side of the ions trajectories. This detector amplifies the number of electrons and provides the position and the time signals. Initially planned to be a large micro-channel plates mosaic, this detector was replaced by a low-pressure thin gas chamber principally because of its much lower cost. If simple in its principle, this detector working under 1 MeV per nucleon needed an important R& D effort because of the necessity to reduce the matter quantity i.e. to lower as much as possible the secondary emission foil thickness but above all the entrance window of the detector the 10 keV electrons have to cross. The whole ensemble of the detector is immersed in a large gap magnet dipole providing a magnetic field parallel to the electrostatic one in order that the 10 keV electrons take profit of the 'cyclotron effect' and that they drift from the emission foil to the gas chamber through a 'point to point' optical structure by a matching between the two fields. It can be seen on fig 9 how the resolution is improved when the magnetic field is set to about 100 gauss.

8. Trajectories reconstruction.

Two methods were investigated in order to reconstruct the trajectory of each ion. One is a method developed in MSU for the spectrometer S800 based on the calculation of the 1 rst, 2 nd, 3 rd and any n th order transfer matrix , followed by an iterative inversion of the transfer matrix using the code 'Cosy infinity '. In our case it seems that it should be necessary to go to 5 th order.
The second method developed at GANIL (see ref. 6) is the following:
It is based on the construction of a database of trajectories (10000), which allows a mapping of the whole phase space, like a 'reference grid' followed, by a comparison with the measured parameters..
In practice we have:
4 quantities to be reconstructed:

$B\rho$ the magnetic rigidity,

θ_i and Φ_i the two emission angles

y_i the vertical position

4 measured final coordinates:

x_f and y_f the final horizontal and vertical positions

θ_f and Φ_f the final horizontal and vertical angles.

we try to solve:

$$x_f = x\,f\,(B\rho, \theta_i, \Phi_i, y_i)$$
$$y_f = y\,f\,(B\rho, \theta_i, \Phi_i, y_i)$$
$$\theta_f = \theta\,f\,(B\rho, \theta_i, \Phi_i, y_i)$$
$$\Phi_f = \Phi\,f\,(B\rho, \theta_i, \Phi_i, y_i)$$

(we assume that $x_i = 0.0$)

For each ion if $(B\rho, \theta_i, \Phi_i, y_i)$ is reconstructed, its path length $S(B\rho, \theta_i, \Phi_i, \Phi_i)$ can be interpolated within the grid to obtain its velocity using the measured time of flight Tof as follows:

$v = S(B\rho, \theta_i, \Phi_i, y_i) / Tof$ allowing the calculation of the quantity:
$M / q = B\rho / v$
The grid is calculated using the predictive TOSCA code or the measured field map and it can be even corrected by calibrations obtained with a beam the $B\rho$ is well known, sent through a grid with holes defining initial angles and located just behind the target.
The results of the simulations obtained by using a TOSCA map are shown on figure 10. The expected resolution around 10^{-3} depends on the (θ_i, Φ_i) region.

9. Reactions simulations.

One example of simulation involving all the optical elements, i.e. the quadrupoles,the velocity filter and the dipole, (see ref.2)
Fig 11 shows the simulation of the 160 Gd (8He, 165 Dy) 3n reaction at 32 Mev total energy, in the mass spectrometer (A / Q) mode, (number 3).

The set up of the spectrometer is the following : for the Wien filter: E = 200 kV / m and B = 2.0 kG and for the spectrometer dipole: B = 1.34 kG i.e. $\theta = 22°$. In this specific case the velocity dispersion provided by the Wien filter is matched with the inverse one given by the dipole, in order to be achromatic in position at the focal plane location. We can see that the separation between masses 163, 164, 165 is well achieved.

10. First results.

Tests achieved with an alpha source and presented in paragraph 5, consisting in the measurement of the position and the angle in the focal plane for three magnetic rigidities to illustrate the efficient aberrations correction have been pursued by an experiment in November looking at the elastic scattering of a beam of 13 C at 15.5 MeV / u on a gold target. The very preliminary results obtained with the standard detection, two drift chambers and plastic, concerning the angular resolution are very promising. The fig 12 shows the horizontal measured angles on the focal plane and the drift time measured in the drift chamber 2, i.e. the vertical position of ions in this chamber. For these measurements the initial angles at the target exit were fixed by a grid equipped with a series of 1 cm spaced and 1mm diameter holes (along two horizontal and vertical directions). The angular resolution in θ is about 4 mr at fwhm.
A complete analysis of data obtained from this first beam test is going on.

11. Conclusion.

Through this short paper we have briefly presented the status of VAMOS and only emphasized the topics which in our opinion needed a huge R&D effort. The first tests with beam have given very promising results and we consider the spectrometer is now ready to be run very soon.

References:

1. W. Mittig and al. Memorandum of Understanding for the construction of VAMOS, internal report, 18 June 1998,
2. http://www.ganil.fr/vamos
3. H. Savajols and M.Duval. Correction of aberrations in the Q2 quadrupole. GANIL internal report
4. M. Malard and al. VAMOS Velocity Filter: INP Orsay internal report –April 1999-.
5. C.Mazur and al. A gas Secondary Electron Detector: DAPNIA/SPHN-99-59 CEA/SACLAY-DSM report.
6. B. Jacquot. VAMOS aberrations study and trajectories reconstruction. GANIL internal report.

Figures captions:

1 layout of the whole ensemble of the spectrometer.

2 positions (x) and angles (t) measured in the focal plane detectors perpendicular to the beam trajectory before aberrations correction.

3 positions and angles after a theoretical multipolar correction.

4 shape of the poles of the quadrupole Q2.

5 a positions and angles after correction of the aberrations.

5 b results obtained with a three picks alpha source

6 cross section of the multi-electrodes electrostatic tank: view of the high voltage equi-potentials (right half part).

7 general layout of the detection.

8 view of the SED detector.

9 resolution of the SED, with and without magnetic field.

10 magnetic rigidity resolution versus trajectories angles.

11 simulation of a reaction in the mode 'mass separation'.

12 angular calibrations.

Photo 1: Wien filter: view of the multi-electrodes electrostatic tank inside the dipole.

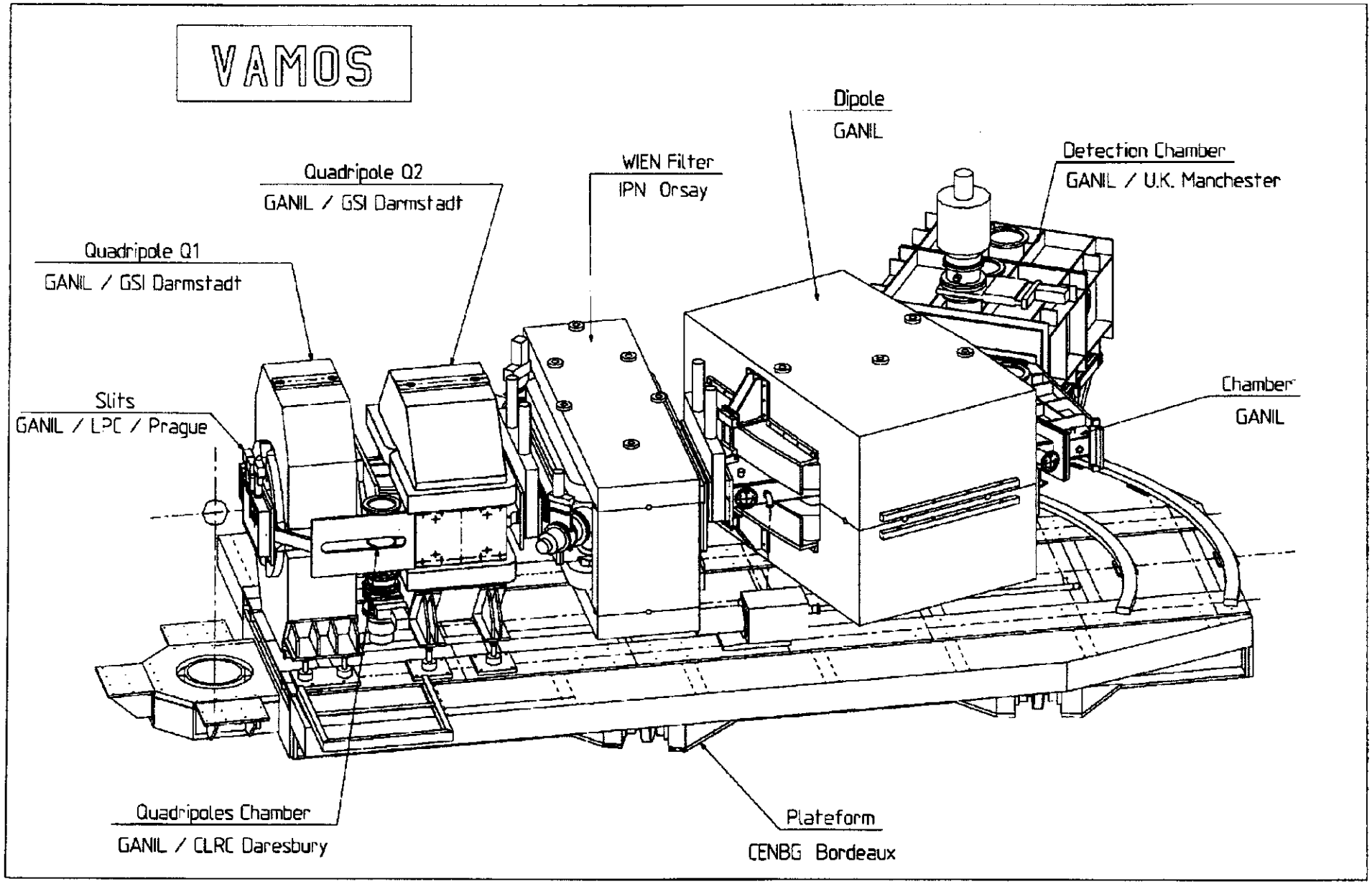
VAMOS
Dipole
GANIL
Detection Chamber
GANIL / U.K. Manchester
WIEN Filter
IPN Orsay
Quadripole Q2
GANIL / GSI Darmstadt
Quadripole Q1
GANIL / GSI Darmstadt
Slits
GANIL / LPC / Prague
Chamber
GANIL
Quadripoles Chamber
GANIL / CLRC Daresbury
Plateform
CENBG Bordeaux

fig: 1

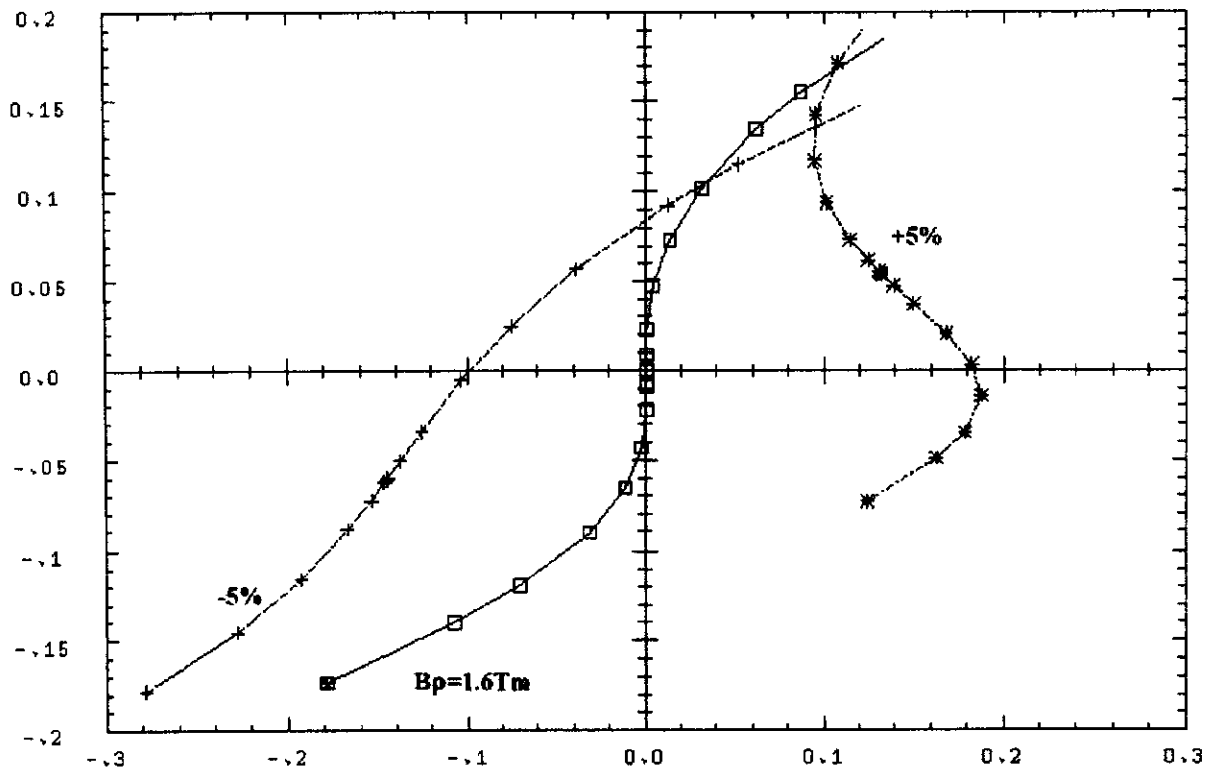

Figure 2:aberrations in the focal plane x-t before corrections

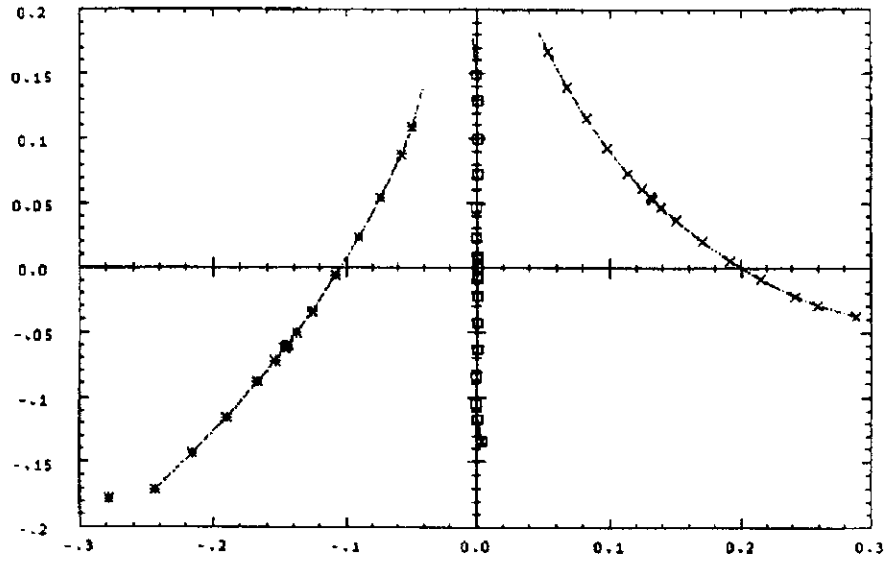

Fig 3 : multipolar correction

Position in the focal plane for ions ranging from - 160 mr to +160 mr. Central trajectory, ions with BR = 1.6 T.m, on the left BR*1.05, and on the right BR*0.95.

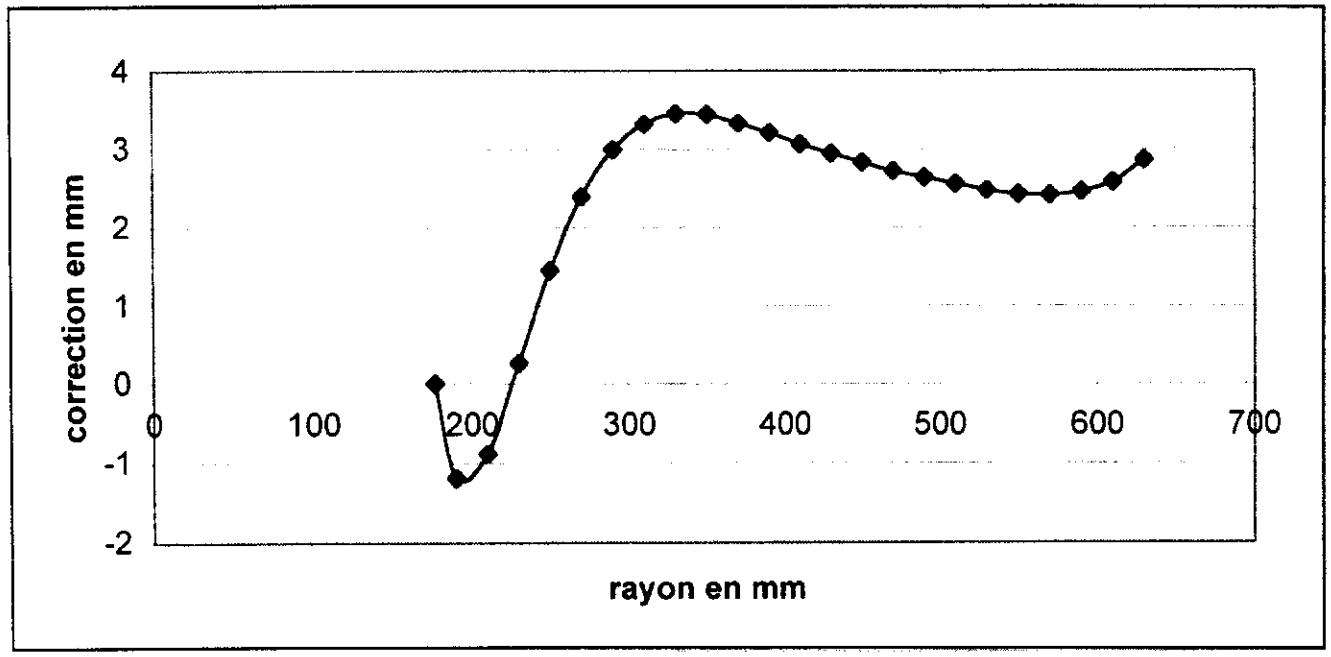
correction en mm
4
3
2
1
0
-1
-2
0
100
200
300
400
500
600
700
rayon en mm

Fig 4

Theory

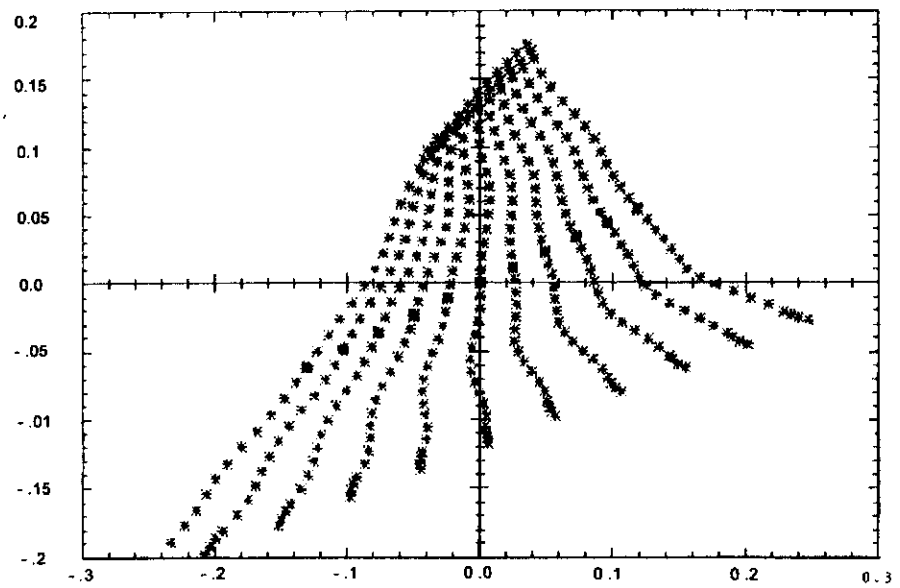

Fig 5 a

Experiment

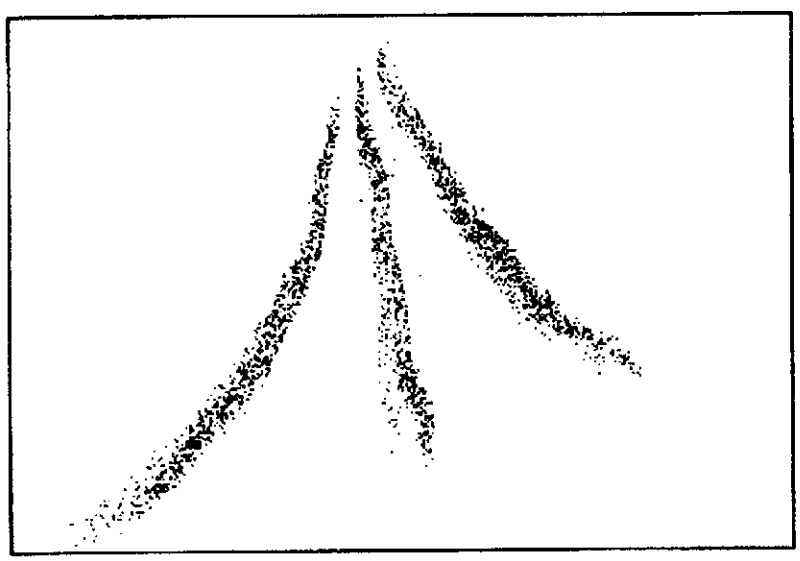

Fig 5 b

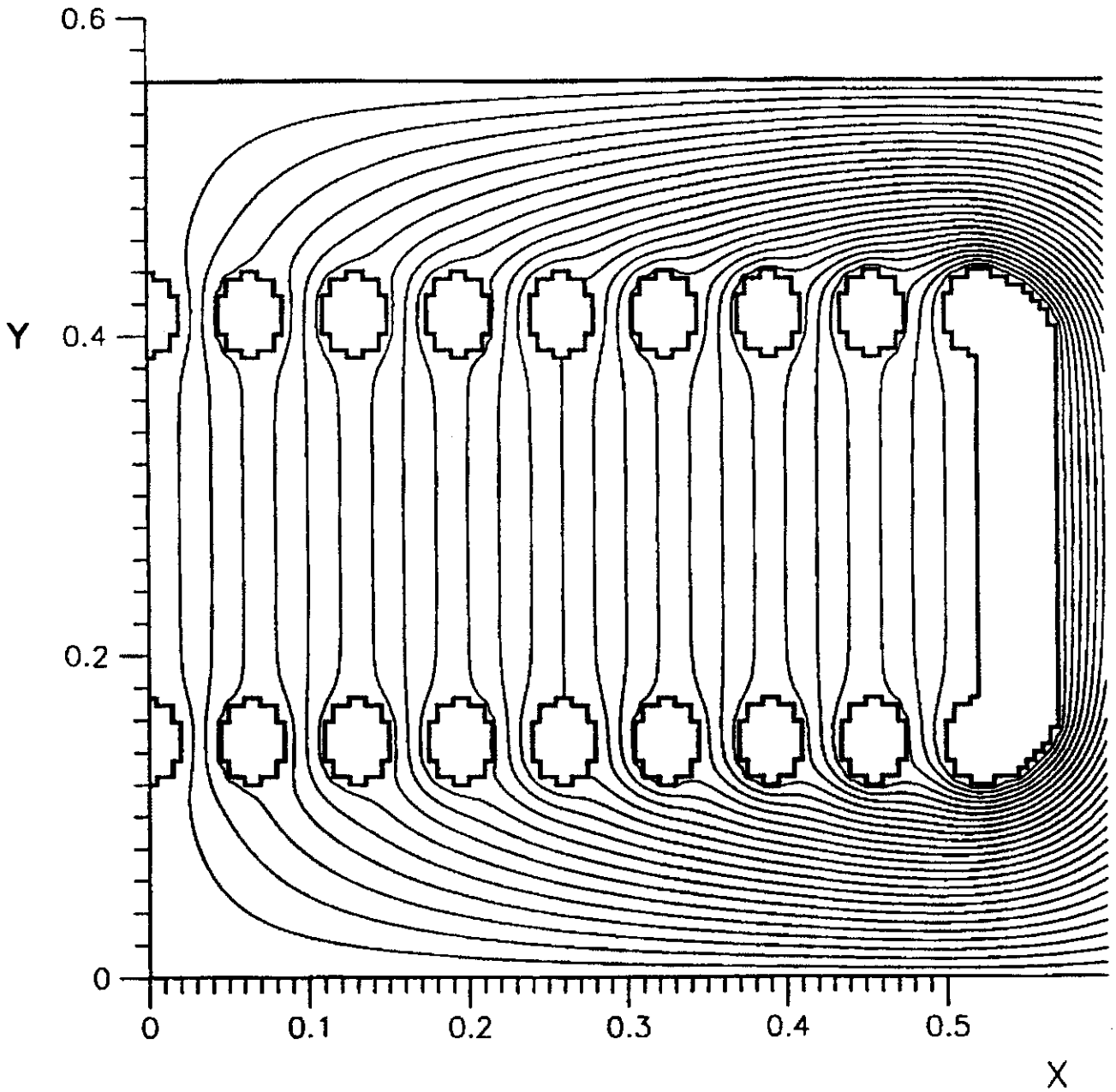

Fig 6

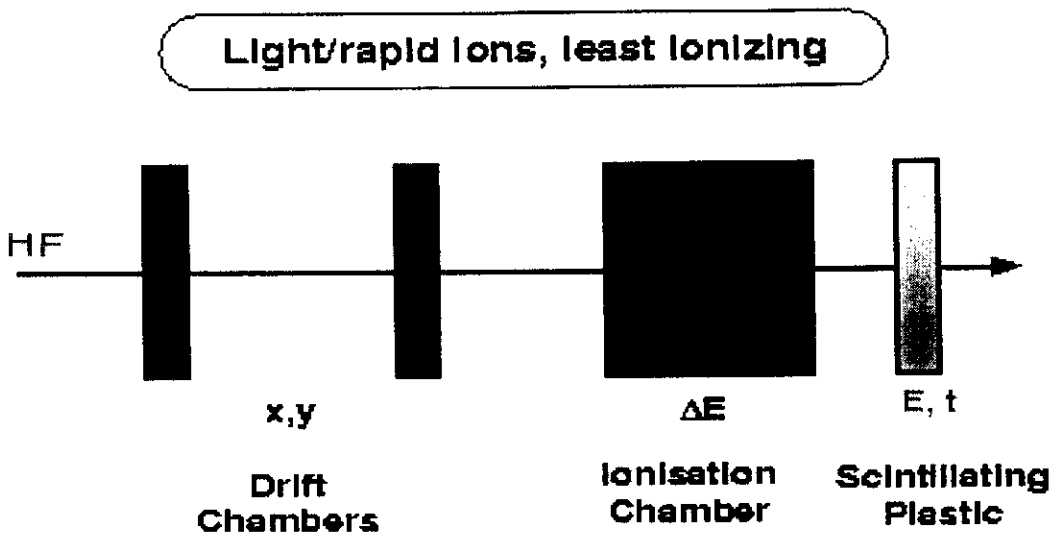
Light/rapid ions, least ionizing
HF
x,y
ΔE
E, t
Drift Chambers
Ionisation Chamber
Scintillating Plastic

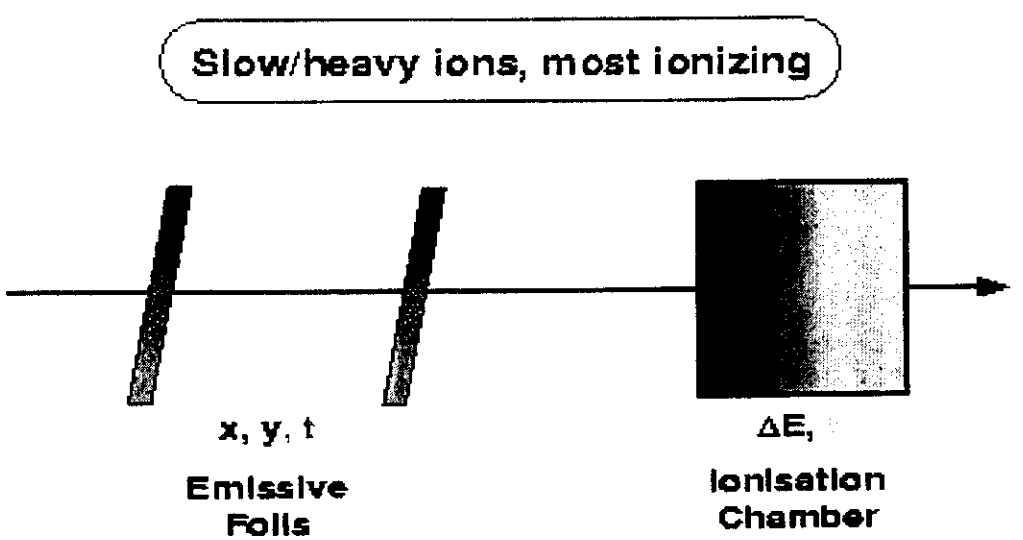
Slow/heavy ions, most ionizing
x, y, t
ΔE,
Emissive Foils
Ionisation Chamber

Fig 7

Secondary Electron Detector inside VAMOS Spectrometer

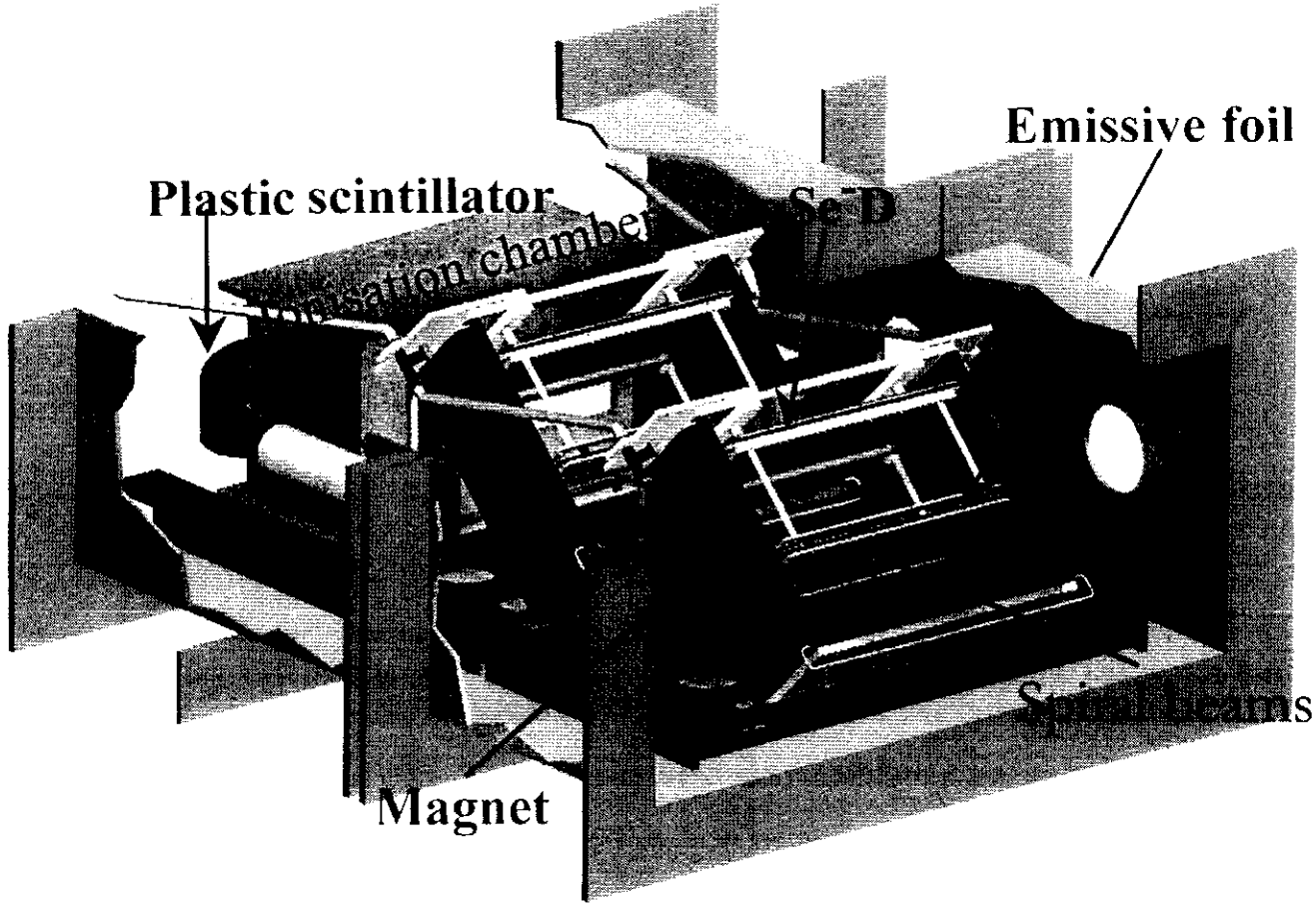

Fig 8

SED : Va = 520 Volts - 4 Torr C4H10

Feuille émissive collimatée par 2 trous de 1.2 mm de diamètre

<u>Position des trous:</u> +/-3 mm par rapport au centre

Fit gaussien +/- 2 pistes

E= 10 kV / B = 0 gauss

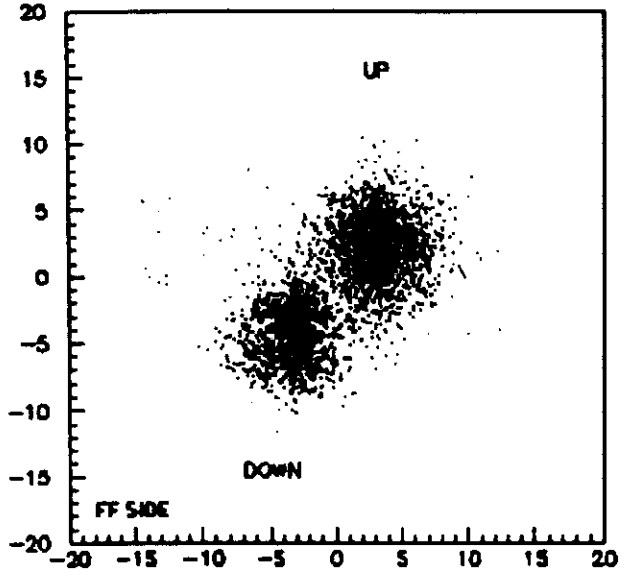

Résolution (FWHM): X=3.7 mm - Y= 4.8 mm

E= 10 kV / B = 100 gauss

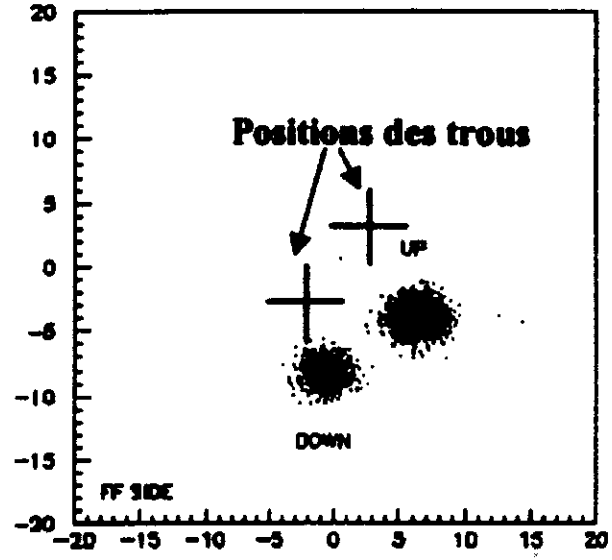

Résolution (FWHM): X=1.3mm - Y= 1.8mm

P. Bourgeois - C. Mazur

Fig 9

SIMULATED
RESOLUTION
(Bρ)
Angular dependance

Simulation :
sample --> 20000 trajectories
Resolution of Detection :
0.25 mm in X and Y (FWHM)
1.0 mrd in θ and φ
Beam size on the target :
2mm x 2mm
Target's thickness : 0.02mm

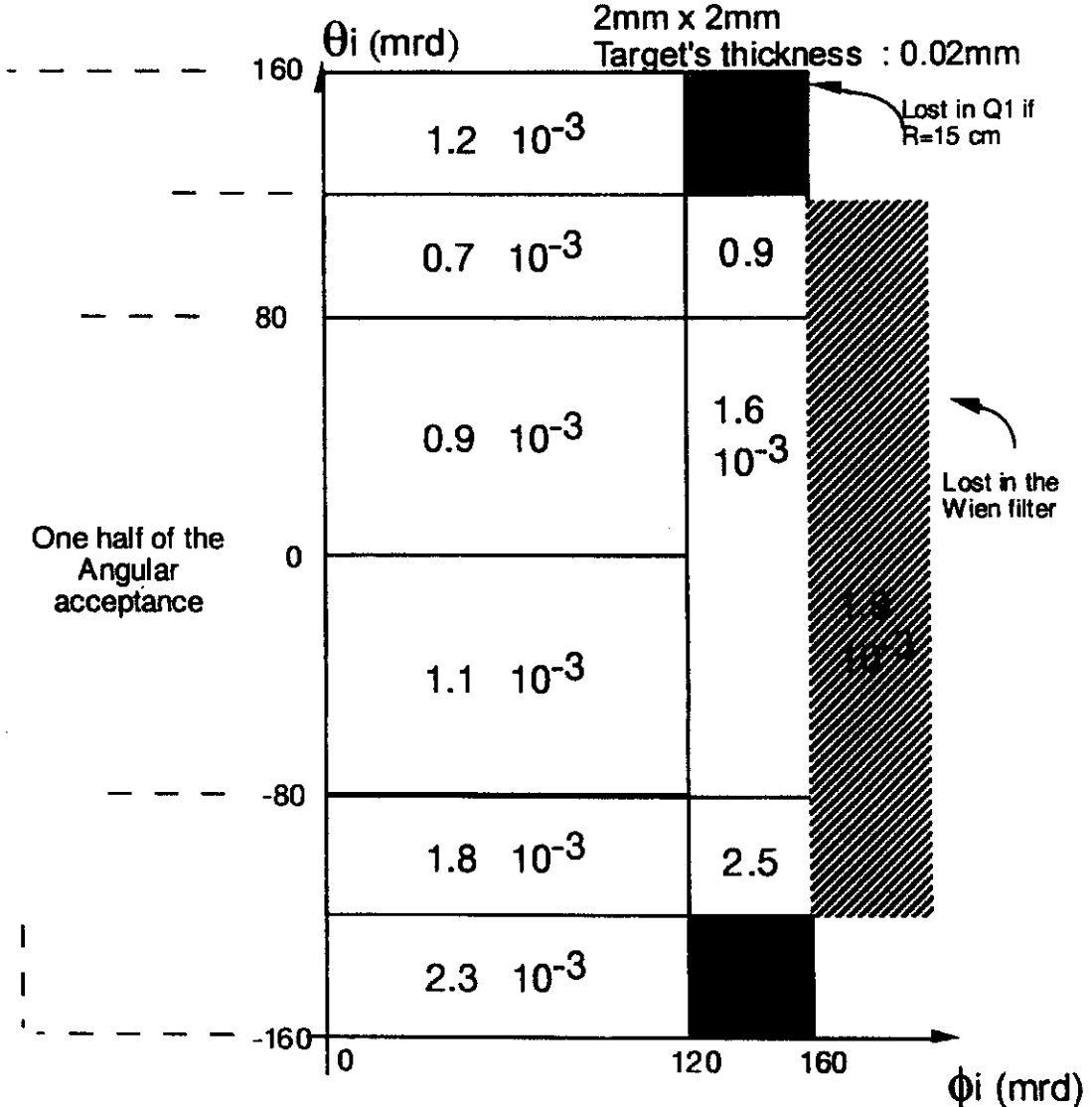

TOTAL ANGULAR ACCEPTANCE =0,085 str
Reconstruction :
MEAN RESOLUTION IN Bρ (FWHM) = $1.4\ 10^{-3}$
IN $\theta_{initial}$ = 2. mrd
IN $\phi_{initial}$ = 8. mrd

Fig 10

Wien filter : E = 200 kV/m
B = -0.20 T

Dipole : B = 1.34 kG
θ = 22⁰

Bρ = 0.5517 Tm, ΔBρ = +/- 5%,
Δθ = +/- 10mrad, Δφ = +/- 160mrad

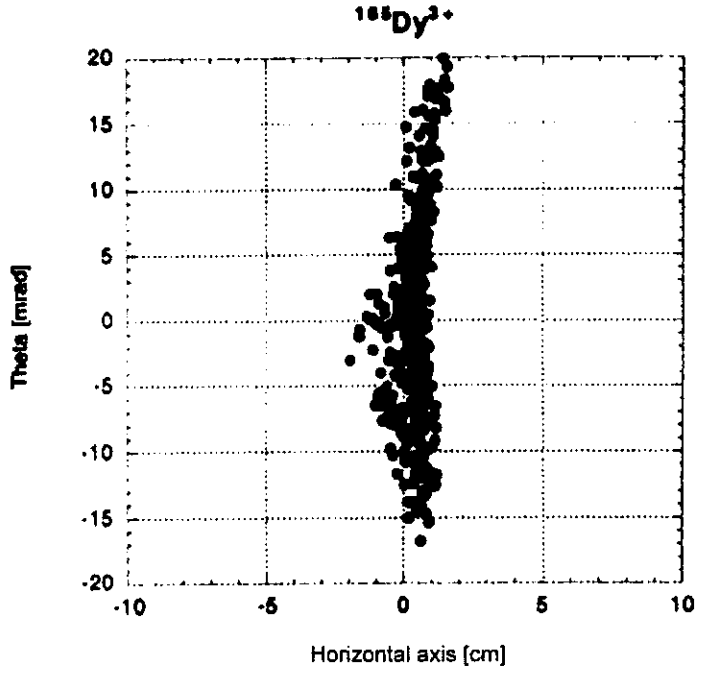

Nucleus	Q	σ[mb]	Bρ [Tm]
^{164}Dy	3+	10	0.5665
^{165}Tb	3+	3	0.5690

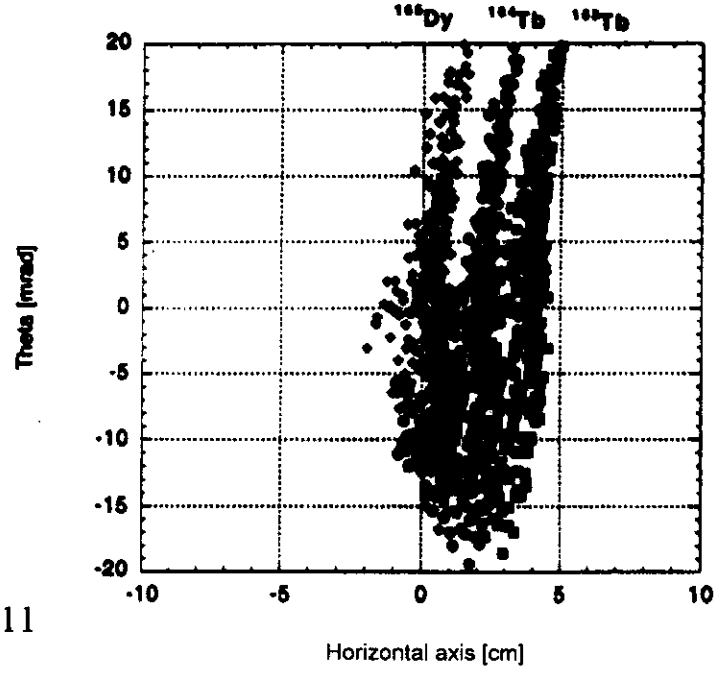

Fig 11

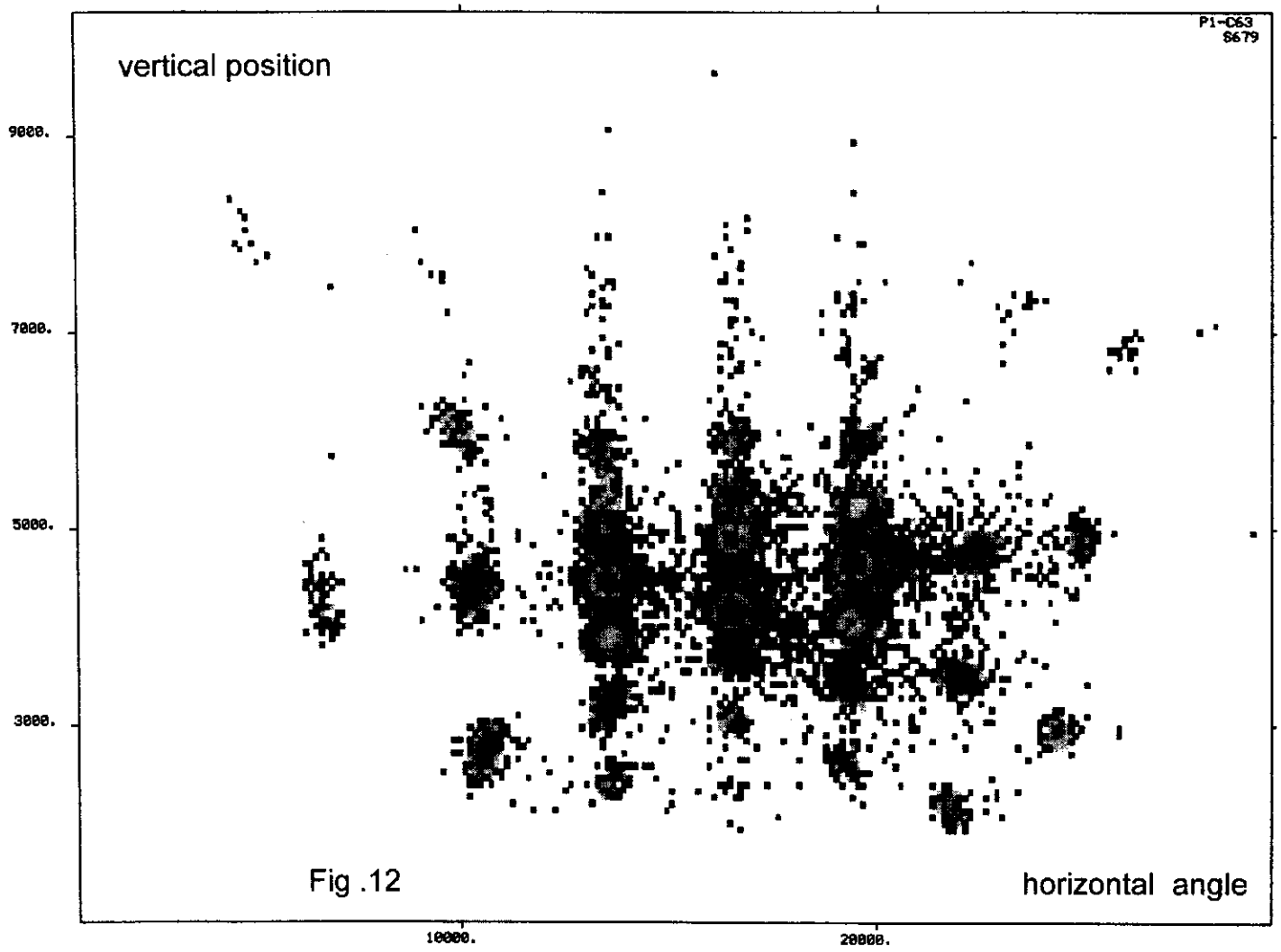
P1-C63
S679
vertical position
9000.
7000.
5000.
3000.
10000.
20000.
horizontal angle

Fig .12

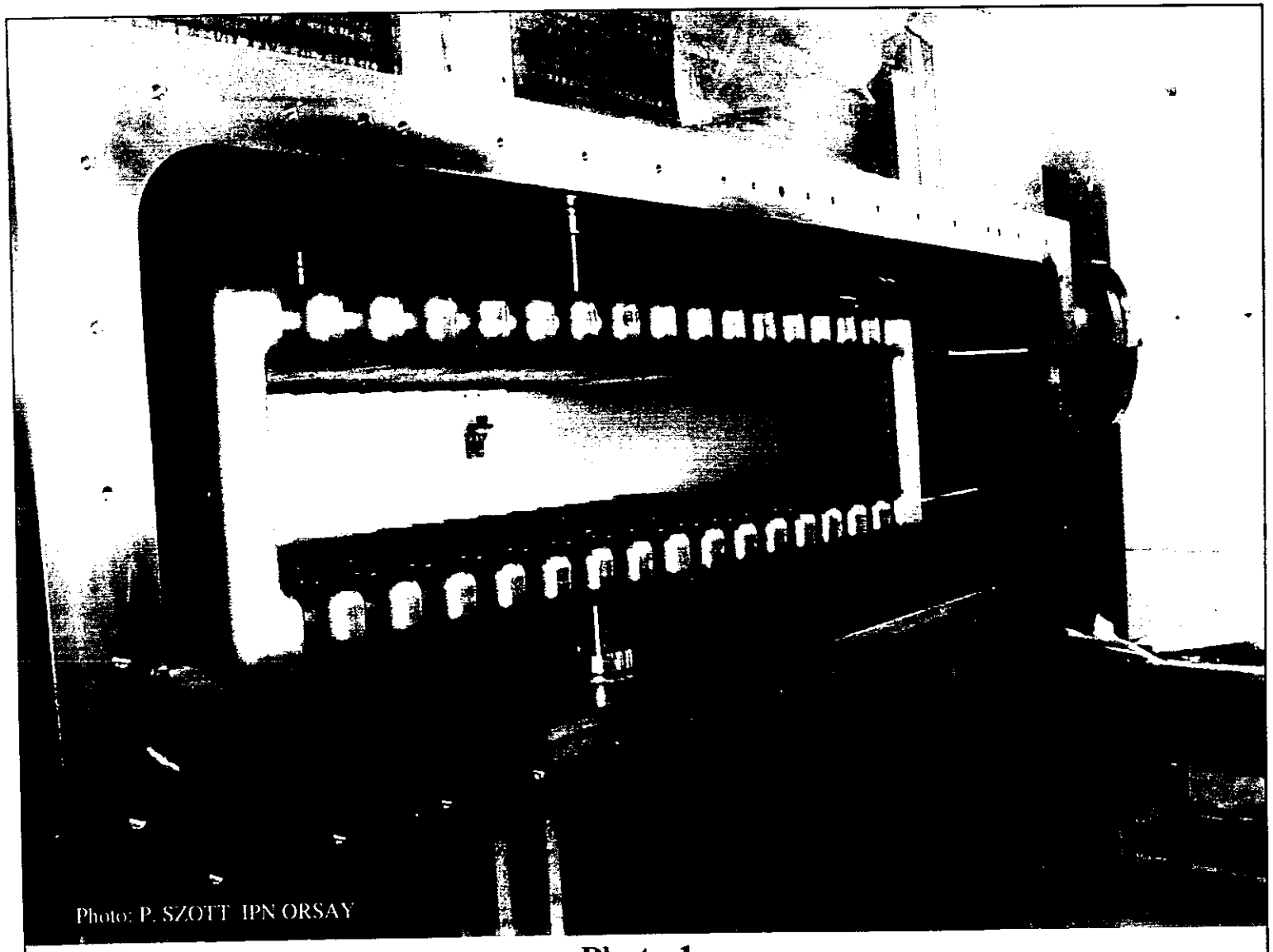

Photo 1